Trend removal from Electrochemical Noise data

M. Ohanian, V. Martínez–Luaces, V. Díaz

Facultad de Ingeniería – UDELAR. J. Herrera y Reissig 565, C.P. 11300.

Montevideo, Uruguay

mohanian@fing.edu.uy

Abstract

Three trend removal methods were performed over computational simulated

data. Their performance was evaluated by sequence dependent and

independent statistical analysis. Polynomial fitting, moving average removal

(MAR) and moving median removal (MMR) were used for trend removal. It was

concluded that the MMR method yielded the best results for the simulated

signals. In order to evaluate these methods with experimental data, the

electrochemical noise (EN) technique was employed to characterize – ex situ –

corrosion products from low alloy steel under atmospheric corrosion

conditions.

Keywords: electrochemical calculation; electrochemical noise; simulation

1   Introduction

The electrochemical noise (EN) technique measures fluctuations in potential and/or current, produced by variations in electrochemical kinetics. An advantage of this corrosion monitoring technique is that no external signals are required, so the system is characterized under free conditions. Furthermore, the apparatus is more affordable than other electrochemical techniques [1]. Application of the EN technique yields information on corrosion process mechanisms, kinetics and morphology [2] from the calculation of the parameters of noise resistance ($R_N = \frac{\sigma_V}{\sigma_I}$), localization index ($LI = \frac{\sigma_I}{I_{RMS}}$), and power spectral density (*PSD*).

EN provides information in terms of current and potential fluctuations of low amplitude and frequency. The term 'drift' could be defined as a temporal change in the average of the measured parameters. The definition of drift is very close to that of EN: in fact, the difference between drift and EN is diffuse.

Drift implies the existence of a non-stationary signal at least within the measurement time. In these conditions, EN statistical analysis from the point of view of sequence independent (calculation of standard deviation) or sequence dependent (calculation of power spectral density) analyses becomes invalid.

Instability in the response of the test electrode during the experiment is

frequently found in other electrochemical techniques such as electrochemical

impedance spectroscopy (EIS). The origin of the drift is found in

electrochemical phenomena with a duration that exceeds the maximum

experimental time, in the diffusion of reactive or corrosion products toward or

away from the interface, in the dissolution of corrosion products and in wetting

phenomena.

K. Hung Chan et al [3] developed some theoretical aspects of the trend removal

problem. They established the difference between the most popular trend

removal methods, i.e., first differences (so-called point to point) and least

square regression. The authors proved that under linear trend and white noise,

the first difference filter generated an exaggerated power spectral density

(PSD) at high frequency and attenuated PSD at low frequency. On the other

hand, the regression residuals exhibited exaggerated PSD at low frequency and

attenuated PSD in the high frequency region.

Mansfeld et al. [4] carried out a theoretical and experimental study of the

effects of trends in noise fluctuations. They applied a linear fit method to the

trend from experimental data. As a result, the authors obtained good

agreement between the spectral noise plots after trend removal and impedance

spectra determined at the same exposure time. They concluded that the

moving average removal method (MAR) proposed by Tan et al. [5], generated

erroneous results.

Bertocci et al. [6] analysed the performance of commonly used trend removal

methods, i.e., MAR, polynomial fitting, digital high pass filtering and analogical

high pass filtering. The methods were applied on simulated data obtained by

overlapping white noise and linear trend. The authors examined the influence

of box size on the MAR method, concluding that using a small MAR box size

effectively removes the drift without phase shift, but also removes a large part

of the low frequency components of the signal. On the other hand, a high

order MAR method generates artefacts in the signal shape. Analysing the

polynomial method, the authors presented the attenuation produced by

polynomials of different orders, for different experimental periods. The 5th

polynomial order was effective for the elimination of the components of

frequency $1/T$ and $2/T$ (where T is the experimental period) but the best

results were achieved when the polynomial method was combined with

prepossessing windowing (Hann window). The digital Chebyshev window of

different cut-off, retrieving the white noise PSD after applying a high pass (HP)

filter, was also performed. The authors considered that HP analogical filtering

is the ideal way to eliminate low frequency components of the signal. However,

active filters of cut-off frequency close to $1/T$ and low intrinsic noise are too

expensive. Moreover, the greatest drawback of analogical filtering in real time

is that the components are subjected to large oscillations when the signal

suddenly varies, such as when switching the system on.

In a previous work [7] Ohanian et al. found excessively high dispersion for

experimental EN results for low alloy steel in sodium sulphate solution. They

ascribed this excessive EN dispersion to the detrending data method

employed. Working with simulated data they studied the influence of the

polynomial detrending step and the aliasing phenomena, and they confirmed

that the trend removal method employed was the principal cause of the

excessive dispersion in the EN parameters. Polynomial fitting was compared

with the back first differential method, Butterworth filtering (Matlab® Signal

Processing Toolbox©) and a method proposed by the authors: median interval

cubic splines (MICS). The MICS method, showed the best training performance.

In this method a group of points (nodes) were obtained by dividing simulated

data into n equal intervals, and computing the average time and position

within the interval. These nodes were matched using cubic splines. Finally,

noise was calculated as the difference between the simulated data and the

interpolated trend.

Another method proposed in the literature utilizes Artificial Neural Networks (ANN) in connection with Data Simulators for detrending. ANN was successfully used for traditional Noise Filtering in a wide range of areas. In a previous study of ours (Martínez et al. [8], Back propagation ANN was trained with simulated data, and as a result, a good level of predictive ability was obtained in the case of Lorentz's function with Gaussian-distributed noise. Indeed, we found that in ANN detrending, especially at high frequencies, there was no influence on the superimposed signal. These results and PSD validation were published [8]. However, we found that when the degrees of freedom increased, poor results were obtained, mainly in the low frequencies domain, in the case of trend and/or using non-Gaussian distributed noise. Moreover, with increasing difference between trend and noise, the method became less accurate. The use of ANN in real data, with non predictable trend shape, would require a variety of training curves or pre selection of the network to be used.

The aim of this work was to analyse the performance of three methods of trend removal, i.e., polynomial detrending, moving average removal (MAR), and moving median removal (MMR). The signals analysed were simulated data sets with different and non-trivial tendencies. The noise employed was a discrete transient of exponential decay that simulates a non-stationary pit. Finally, the detrending methods were also applied in order to characterize protective

properties of the corrosion products formed in low alloy steel (in sodium

sulphate media) exposed to atmospheric conditions in an Antarctic site [9] for

one year.

2   Materials and methods

2.1   Noise simulation

Two EN data sets were generated by adding simulated noise data and two

different trend lines.

In all cases the interval between data points was 0.7 seconds.

Noise: the noise consisted in a pulse train with an amplitude corresponding to

a uniform distribution of [0, 2.5). Initial time was obtained from a binomial

distribution of 0.02 and its sign had a binomial distribution of 0.5.

The pulse function used could be expressed as:

$$f(t) = A\,B\,t\exp\!\left(-b(t-c)^d\right) \tag{1}$$

Parameters *b, c* and *d*, were adjusted in order to obtain a signal similar to a

representative experimental transient. Factor *A* represented the amplitude and

parameter *B* adjusted the sign function.

2.2 Trend simulation

Functions used as trend lines in simulation processes must be non- trivial.

Polynomials, sinusoids and exponentials, among others, can be considered as

trivial, because they can be easily approximated by elementary mathematical

methods. This is an important issue to be considered when testing trend

removal methods.

Here, we used the following curves as trend lines:

Curve 1

$$f(t) = \frac{ac^{t/3}}{\Gamma\left(\frac{t}{3}+1\right)} - b \qquad (2)$$

$$\text{Where} \quad \Gamma(x) = \int_{0}^{+\infty} t^{x-1}e^{-t}dt \qquad \text{Euler's Gamma function} \qquad (3)$$

Curve 2

$$f(t) = y_0 + \frac{2A}{\pi}\frac{w}{4(t-x_c)^2 + w^2} \qquad \text{Lorentz's function} \qquad (4)$$

Two signals were obtained by the addition of noise function to curve functions:

Simulated signal 1: Noise plus Curve 1; Simulated signal 2: Noise plus Curve 2.

The simulated pulse train and the simulated signals are represented in Figure 1

(a) and (b); parameters were fitted in order to obtain curves with similar power

trend lines.

Simulated signals and noise spectra obtained by the maximum entropy method

(MEM – 15 order, ENAnalize® program) are presented in Figure 2. The order of

the MEM method applied affects the power spectrum that is obtained. If the

order is small the obtained spectrum is smooth, while with high MEM order the

spectrum appears much noisier. When using the MEM with relatively low order

[2], comparison of the spectra obtained by applying different detrending

methods is easier. Fast Fourier Transformed (FFT) provides more reliable

results, but the spectra obtained are noisy and thus the representation of PSD

results in the same graphic with comparative aims, is not clearly depicted thus

PSD results for FFT cannot be compared clearly with the MEM results, and are

not shown in Figure 2.

2.3   Experimental signals

The probes – low alloy steel in flat geometry – were prepared and exposed in

atmospheric conditions, according to guidelines agreed in the Atmospheric

Corrosion Iberoamerican Map (Spanish acronym MICAT) project, experimental

details of which can be found in the literature [9]. Specifically, the probes

analysed were exposed for one year at the Uruguayan Antarctic Base (Lat: 62°

10'S, Long: 58° 50'W, Elevation: 17.2 m OSL, SO_2:<0.05 mg day^{-1}m^{-2}, Cl^-: 160

mg day^{-1}m^{-2}). For this period, the time of wetness (RH>80%, temperature> 0

°C), expressed as annual frequency, was 0.354. Corrosion penetration in the

substrates, measured by a gravimetric method, was 66 µm/yr [10–11].

Finally, the corrosion products were characterized ex–situ by electrochemical

methods (EN) and scanning electron microscopy (SEM).

Electrochemical runs were performed using a three–electrode compartment cell

with three electrodes: saturated calomel reference electrode (SCE) with a

Luggin–Haber capillary tip, working electrode (WE) and counter–electrode (CE)

of low carbon steel. The temperature for all runs was 20 ± 2 °C. Sodium

sulphate 0.1M was employed as the supporting electrolyte.

 The potential of the WE against the SCE and the current between the WE and

CE were recorded every 0.7 seconds using the electrochemical interface ACM

Gill8AC. Each run lasted for one hour. Potential values in the text are given on

the saturated calomel reference electrode (SCE) scale.

2.4   Trend removal methods

Three different drift removal methods were evaluated: Polynomial fitting (9–order), MAR, and MMR.

➢ Polynomial fitting (9–order)

This is a widely utilised method. The trend is fitted using least squares regression. The noise is computed as the difference between experimental and predicted data (by the regression model). In this case, a nine–order polynomial was utilised. The order of the detrending polynomial allows a cut–off frequency of approximately $1/T$ [7], in this case 3×10^{-4} Hz.

➢ MAR–10

In this method, the noise is computed as

$$x_{n} - m_{n} \qquad (5)$$

where x_{n} denotes the n–th simulated value and m_{n} represents the following moving average:

$$m_{n} = \frac{1}{21} \sum_{p=-10}^{10} x_{n+p} \qquad (6)$$

Bertocci et al. [6] presented the transfer function for MAR–p:

$$H_{\mathrm{MAR}}(f) = 1 - \frac{1}{2p+1} \frac{\sin\left([2p+1]\pi\,{}^{f}\!/_{f_{s}}\right)}{\sin\left(\pi\,{}^{f}\!/_{f_{s}}\right)}, \qquad (7)$$

where f_s represents the sample frequency. The useful frequency range, within which the spectrum is not attenuated, is between $f_{max}/(2p+1)$ and f_{max}. The highest frequency is the Nyquist frequency ($f_{max} = f_s/2$). In our case the interval used was between 3.4×10^{-2} and 0.7 Hz.

> ➢ MMR-10

MMR is equal to the MAR method, except for the substitution of the moving mean by the moving median. In this method, the noise is computed as

$$x_n - k_n \qquad (8)$$

where x_n denotes an experimental value and k_n represents the moving median:

$$k_n = median\left[x_{n-10}, \ldots, x_n, \ldots x_{n+10}\right] \qquad (9)$$

3   Results and discussion

3.1 Simulated signals

The Simulated Noise data set had a mean of −0.0112 and standard deviation of 0.3736. *Table 1* shows the statistical results for the trend removal methods employed for simulated signals 1 and 2.

With all the methods performed, the noise mean value reported was close

nearby to zero (*Table* 1). Consequently, it was not possible to come to any

conclusions about the performance of the drift removing methods taking only

this parameter into consideration.

Figure 2 shows the spectra of the simulated signal, the original simulated

noise and those obtained for the detrending methods employed.

The simulated noise data presented a spectrum with white noise in the low

frequency region with amplitude 0.5. This value is coincident with the transient

mean amplitude. At 0.04 Hz the spectra had a break point, the linear shape

has a slope of -2.6 dec/dec (roll-off slope). The frequency of the break point

calculated according to Cheng et al. [14] was 0.08 Hz (inverse of

2*PI*transitory period) and the PSD break point was 0.2 (2*pit initiation

rate*mean amplitude*transitory period).

> ➢ 9-order polynomial

The standard deviations are presented in *Table 1.* For Signal 1 – with a

smoother trend – the standard deviation is close to the original noise

dispersion. For Signal 2, the method gives a standard deviation greater than

the original one.

The spectra confirm this behaviour: for Signal 2 the polynomial method does

not remove the power in the low frequency region. The spectrum obtained for

Signal 1 is a good reproduction of the trace of the original simulated noise.

Thus, it is clear that this detrending method is strongly dependent on the

simulated trend curve, and in contrast to what has been stated by other

investigators in recent published papers [6], in the conditions of this study, we

found it was not a reliable pre-processing method.

➢   MAR-10

This method was not significantly dependent on the trend curve employed

(Table 1). In fact, the standard deviation of the data was not very different from

that of the simulated noise. Analysing the spectrum it can be stated that the

noise obtained fit rather well to the original noise at high frequencies.

However, for lower frequencies (below 0.01 Hz), there was a maximum at ca

0.07 Hz and a plateau was reached, with smaller power values than the original

noise. The frequency breakpoint value obtained after processing the original

noise spectrum data with the MAR method was larger than that predicted by

the interval from the transfer function (7). Summing up, the spectrum

recovered by MAR-10 produced a lower standard deviation value than the

original data.

> ➤ *MMR-10*

In comparison with the polynomial method, both the MMR and the MAR methods were robust to the type of signal processing. The standard deviation obtained by MMR was much closer to the original values than that obtained by the MAR method. The difference between the original value and that obtained by MMR was lower in the case of Signal 1 than in the case of Signal 2. The spectra obtained fit better to the original noise than that obtained by MAR-10 in all the frequency range.

The mean is the most commonly reported statistic of location. However, extreme values will have great influence on it. The mean may not be the most appropriate statistic if there is one value that is much larger or smaller than the other values in a sample [12].

For the calculation of the median, the data must be ordered from the highest to the lowest value. This can be quite time consuming for a large data set and thus calculating the median is computationally more troublesome than calculating the mean for a data set. On the other hand, the median is unaffected by a single (or even several) very large or small numbers [13]. This characteristic is very important when approximating the tendency in an EN data set. In effect, MMR provides a better baseline representation, and then the

subtraction preserves the signal trace, with less attenuation than subtraction of

the mean.

For probability distributions having an expected value and a median, the mean

and the median can never differ from each other by more than one standard

deviation. To express this in mathematical notation, let μ, m, and σ be

respectively the mean, the median, and the standard deviation.

$$|\mu - m| \leq \sigma \qquad (10)$$

$$\mu - \sigma \leq m \leq \mu + \sigma \qquad (10')$$

Besides in the previous inequality, and applying the z-transform, the transfer

function is limited by:

$$H_{\text{MMR}}(f) = 1 - \left(\frac{1}{2p+1} \pm \frac{1}{\sqrt{2p+1}} e^{-2p\pi f/f_s} \right) \frac{\sin\left([2p+1]\pi f/f_s\right)}{\sin\left(\pi f/f_s\right)} \qquad (11)$$

The MMR transfer function has two real roots. Figure 3 shows the transfer

function for the MMR-10 (grey line) and MAR-10 (black continuous line)

methods. Transfer function has a characteristic cut-off frequency of 0.04 Hz

for MMR-10 and 0.07 Hz for MAR-10. MMR transfer function presented

negative values below 0.020Hz, and a strong oscillation nearby 0.7Hz.

3.2   Experimental Signals

Figure 4 shows experimental electrochemical results for current and potential.

Electrochemical *ex situ* analysis were performed in probes that were exposed

in atmospheric conditions. The current data present a trend line – originated

by the differences between the two 'nominally equal' electrodes– with maxima

and values in the range of 0.015 to 0.04 mA. This trend line has superimposed

meta stable pits. The mean pit amplitude is ca. 0.002 mA and their duration is

approximately 3 seconds; their frequency is about every 25 seconds. The pits

have a shape with fast birth and slow decline. The slant of the pit signals is

remarkable, and is clear evidence of surface differences between the electrodes

(asymmetry of electrodes).

The potential curve was smoother than the current signal and presented a

decay trend line from ca. –350 mV to –500 mV vs. SCE at one hour, similar to

signal 1. The amplitude of the voltage noise with respect to the corresponding

signal is significantly lower than that observed in the current signal. Rust

wetting and its corresponding transformation may have been the origin of this

voltage tendency. The potential under –250 mV vs. SCE (an arbitrary limit,

taking into account the evolution of hydrogen in normal conditions about the

cathodic reaction), indicated that the rust formed was not a protective barrier against the corrosion process. The potential transient had an amplitude of ca. 0.1 – 0.5 mV.

Figure 5 shows the spectral density of the experimental data set for (a) the current and (b) the potential and the spectra for polynomial, MAR and MMR treatments.

Ignorance of the 'real' noise makes the analysis of experimental signals difficult. From the shape and amplitude of the current transients, a white noise of amplitude between $4x10^{-6}$ and $2.5 x10^{-5}$ A in current spectra could be predicted. In the same way, a break point close to 0.04 – 0.2 Hz could be expected. From potential spectrum analysis, a white noise with a power of 1 mV and a similar break point could also be predicted. Analysing the poor protection of the rust formed (potential close to –400 mV vs SCE and SEM microphotographs, Figure 6), the surface would be expected to have a low polarization resistance.

The noise obtained by polynomial regression exhibited one plateau below 0.002 Hz and another above approximately 0.08 Hz. The first break point corresponded to oscillations of ca. 500 seconds. It was not clear whether these oscillations corresponded to noise or to a tendency. Their duration and

triangular shape means they are unlikely to have arisen from an

electrochemical phenomenon.

The second break point, 0.08 – 0.1 Hz, agrees approximately with the break

point of the MAR10 and MMR10 treated data, corresponding to the mean

transient duration. Below this frequency value the MMR10 and MAR10 methods

exhibit spectra with amplitude lower than the high frequency plateau (common

to all spectra). The interval of the MAR–10 and MMR–10 detrending methods

employed was 15 seconds. The pits with duration of less than 15 seconds

remained unaffected by both detrending methods. The data results

corresponding to pits with duration of over 15 seconds, showed an altered

shape, with diminished amplitude. This phenomenon is reflected in the

attenuated spectra at below 0.1 Hz for both methods. Transients separated by

less than 15 seconds. This shows the importance of the cut–off frequency

selected when analysing electrochemical processes.

 In the voltage spectrum the polynomial method exhibited the same

performance as was observed after processing the current signal. However,

there was a difference in the trend shape with respect to the treatment in the

current signal. The trend in the voltage spectrum was smooth and similar to

that represented in signal 1. Besides, the polynomial method gave excellent

results with the simulated signal. Thus we would predict that the spectrum

and the corresponding SD obtained with the polynomial treatment are close to

the 'real' situation. For the MAR and MMR methods, the PSD obtained were

similar to those associated with current data processing, with one unique

characteristic. They depicted a signal response which was attenuated in the 0.1

– 0.5 Hz region, with the MMR PSD being lower than that obtained by the MAR

method. The reason may be attributed to the low signal to noise ratio.

Table 2 shows the results of the noise resistance, the ratio of the standard

deviation of voltage and current after the detrending processing with

polynomial, MAR10 and MMR10. In the same table the results for MAR20 and

MMR20 are shown.

$$R_N = \frac{\sigma_V}{\sigma_I} \hspace{4cm} (12)$$

In order to decrease the attenuation at low frequencies, detrending processes

of major step were performed, i.e. MMR–20 and MAR–20, with cut off 0.025

and 0.04 Hz respectively (see Figure 7). In Figure 8 current and voltage signals

processing with MMR–20 were showed.

The change in the cut off method was reflected in the increment of standard

deviation of current and voltage. The deviation ratio, R_N, was not affected.

4　　Summary

Stationary electrochemical noise data is required for the calculation of valid standard deviation and PSD. The trend removal method used affected the processed results. The ideal method should recover most of the signal information without introducing external effects.

The polynomial fitting method has a strong dependence on the trend and presents very good results for smooth tendencies. However; it exhibits rather poor performance in curves with sudden changes of slope and convexity.

The MAR method has robust results with respect to the type of curve analysed. On the other hand, this method alters the low frequency zone of spectra, and consequently the standard deviation results are not accurate. The proposed method, MMR, exhibits a better performance in the simulated signals analysed, however it has the same behaviour as the MAR method in the low frequency zone of spectra.

Based only on the experimental signals, it is not yet possible to establish strong conclusions. It is clear that the polynomial method is not a reliable trend removal technique. On the other hand, MAR and MMR treatments do not offer a definitive solution. In fact, the results suggest that the application of

these methods produces an apparently attenuated response with low noise

signals. In the case of the MMR method, increasing the order of magnitude was

not able to improve its performance in the cases studied.

5   Acknowledgments

6   References

[1]   JR Kearns, JR Scully, PR Roberge, DL Reichert, JL Dawson, Electrochemical

Noise Measurements for Corrosion Applications. ASTM, West

Conshohocken, USA, 1996

[2]   R A Cottis, Interpretation of Electrochemical Noise Data, Corrosion, **57**,

3, pp. 265–285, 2001

[3]   K Hung Chan, JC Hayya, JK Ord, A note on trend removal methods: the

case of polynomial regression versus variate differencing, Econometrica, **45**, 3,

pp. 737–744, 2001

[4]   F Mansfeld, Z Sun, CH Hsu, A Nagiub, Concerning trend removal in

electrochemical noise measurements, Corr Sci., **43**, 2, pp. 341–352, 2001

[5]   YJ Tan, S Bailey, B Kinsella, Factors affecting the determination of

electrochemical noise resistance, Corrosion, **55**, 5, pp. 469–475, 1996

[6]   U Bertocci, F Huet, RP Nogueira, P Rousseau, Drift removal procedures in

the analysis of electrochemical noise, Corrosion, **58**, 4, pp. 337–347, 2002

[7]   M Ohanian, V Martínez-Luaces, G Guineo-Cobs, The Journal of

Corrosion Science and Engineering, (2004) in

http://www.jcse.org/viewpreprint.php?vol=7&pap. Accessed 14th September

2008

[8]   M Martínez, V Martínez, M Ohanian., Data Simulation, Preprocessing and

Neural Networks applied to Electrochemical Noise studies. WSEAS Transactions:

Computer Science and Applications Journal, pp. 810–817, 2006

[9]   M Ohanian et al., Productos de corrosión formados en ambiente marino:

vinculación de variables estructurales y potencial de corrosion, **41**, 3, Rev.

Metal. Madrid, pp. 175–185, 2004

[10]   M Morcillo, E Almeida, B Rosales, J Uruchurtu, M Marrocos (eds):

Corrosión y Protección de Metales en las Atmósferas de Iberoamérica – Parte I–

Mapas de Iberoamérica de corrosividad atmosférica. CYTED, España, 1999

[11]   ISO 9226 'Corrosion of metals and alloys Corrosivity of atmospheres

Determination of corrosion rate of standard specimens for the evaluation of

corrosivity'; ISO, Genève, Switzerland, 1992

[12]   On line document

D Moore, Measures of Location Chapter 3

            http://academic.emporia.edu/mooredwi/rda/notes3.htm. Accessed

28th july 2008

[13]   RL Scheaffer, JT McClave : Probability and Statistics for Engineers Third

            Edition, PWS-KENT Publishing Company, USA, 1990

[14]   YF Cheng, JL Luo, M Milmott, Spectral analysis of electrochemical noiser

with different transient shapes, **45**, 11, Electrochim Acta, pp. 1763-1771,

2000

Figure Captions

Figure 1   (a) Computationally simulated signals, obtained for superposition

of pulse train (simulated noise) on Curve 1 (black line) and Curve 2 (gray line)

(b) Detail of the shape of individual simulated transitory

Figure 2   PSD of simulated signal, simulated noise, and signal treated with

polynomial, MMR10 and MAR10 methods. (a) Simulated signal 1: Noise +

Curve 1. (b) Simulated signal 2: Noise + Curve 2

Figure 3   Transfer function limits for MMR–10 (grey lines), and MAR–10

transfer function (black line).

Figure 4   Time course of experimental current (black line) and potential

(grey line) of EN signals

Figure 5   PSD of experimental untreated signal and signal treated with

polynomial, MMR10 and MAR10 methods for (a) Current data (b) Potential data

Figure 6   SEM images at 500X and 1000X magnification.

Figure 7   Transfer function for MMR–20 (grey line) and transfer function for
MAR–20 (black line)

Figure 8   Current and voltage experimental signals processing with MMR20

Tables

Table 1 Mean and standard deviation for trend removal methods: MAR-10, MMR-10 and 9-order polynomial fitting under simulated pulse train noise (mean: -0.0112, standard deviation: 0.3736)

	MAR-10		MMR-10		Polynomial	
Signal	Mean	SD	Mean	SD	Mean	SD
1	2.49×10^{-4}	0.3204	8.50×10^{-3}	0.3600	-1.39×10^{-5}	0.3735
2	-2.93×10^{-4}	0.3204	5.90×10^{-3}	0.3550	4.13×10^{-3}	1.8261

NOTA: SD is standard notation for "standard deviation"

Table 2 Standard deviation for current and voltage and R_N for experimental signal after applying polynomial, MAR10 and MMR10 detrending methods.

	MAR10	MMR10	Polynomial	MAR20	MMR20
σ_I (mA/cm²)	3.40×10^{-4}	3.40×10^{-4}	5.82×10^{-4}	3.57×10^{-4}	3.47×10^{-4}
σ_v (mV)	0.0664	0.0573	0.155	0.0700	0.0573
Rn (Ω.cm²)	195	168	267	196	165

Figure1 (a)
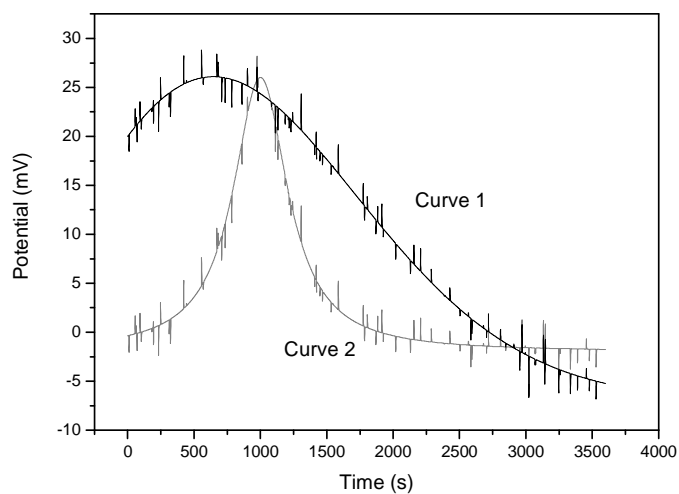
Figure1 (b)
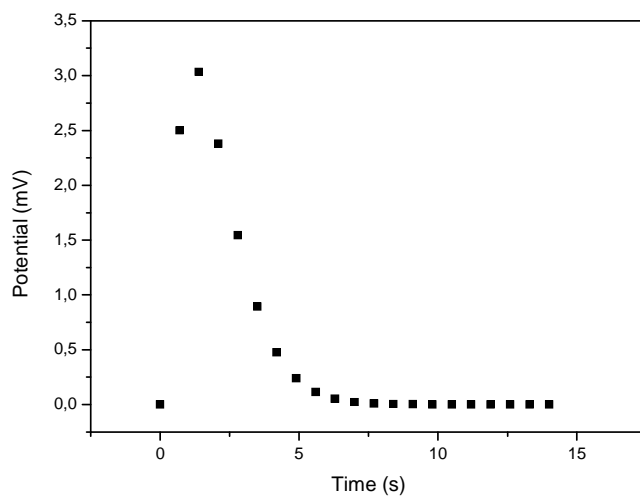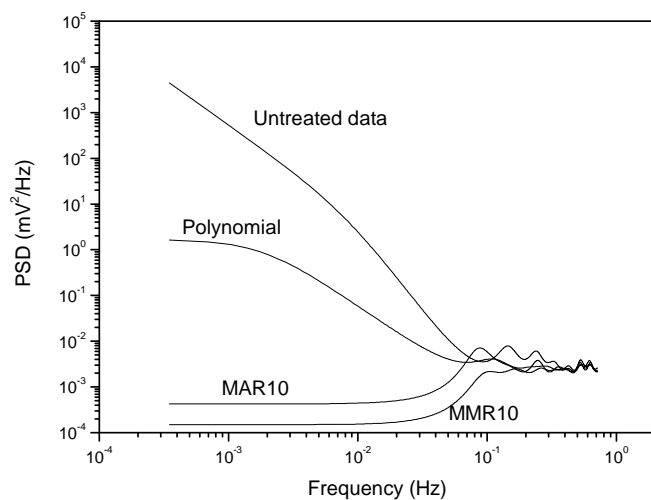
Figure 2 (a)
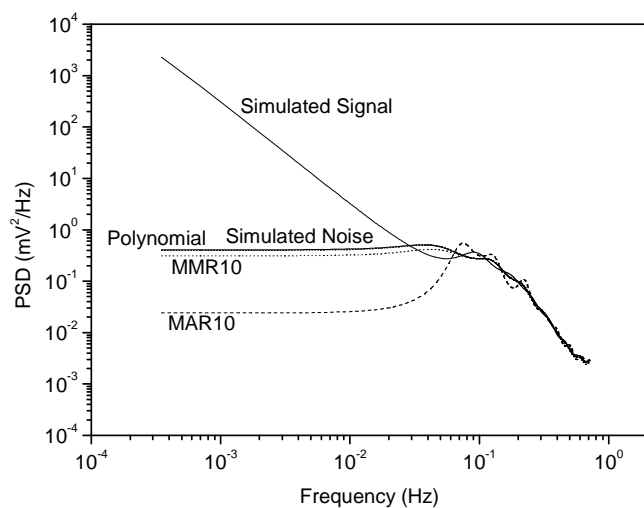
Figure 2 (b)
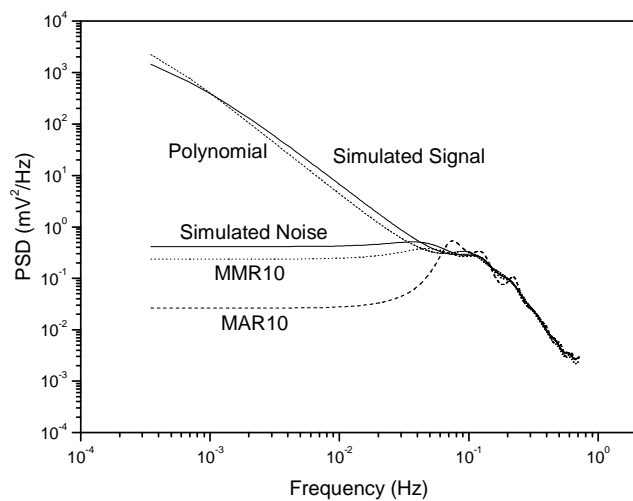
Figure 3
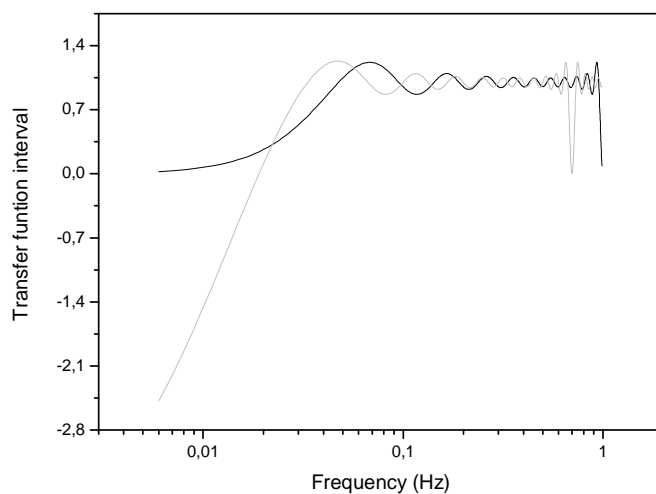
Figure 4
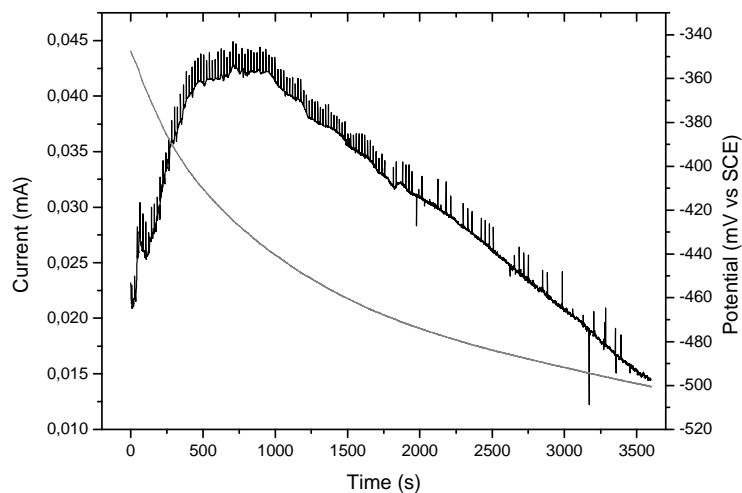
Figure 5 (a)
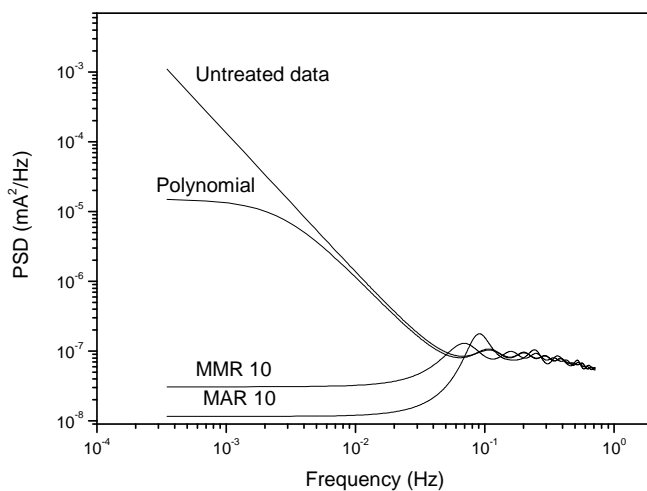
Figure 5 (b)

Figure 6

Figure 7

Figure 8